DE GRUYTER OPEN

Archives of Hydro-Engineering and Environmental Mechanics
Vol. 65 (2018), No. 3, pp. 221–239
DOI: 10.1515/heem-2018-0014

Calculation of Dune Profile Changes Generated by Hurricane: Preliminary Results *

Piotr Szmytkiewicz, Marek Szmytkiewicz, Jan Schönhofer, Michał Morawski, Jakub Malicki

Institute of Hydro-Engineering, Polish Academy of Sciences, 7 Kościerska, 80-328 Gdańsk, Poland,
Corresponding author, e-mail: P.Szmytkiewicz@ibwpan.gda.pl

(Received December 03, 2018; revised January 25, 2019)

Abstract

The paper presents the main theoretical concepts related to methods of calculating the erosion rate for sandy dunes on natural coasts, namely, the beach equilibrium profile and incident waves. To illustrate calculations of dune erosion in the vicinity of the Coastal Research Station (CRS) in Lubiatowo, the *Xbeach* model (an incident wave model) was used. The calculations were carried out for hydrological and hydrodynamic conditions that accompanied Hurricane Ksawery (December 6–8, 2013). The results of the calculations were compared with the measured data. A satisfactory agreement was obtained between the predicted and measured results.

Key words: coastal zone, dune, erosion

1. Introduction

Approximately 75% of the Polish coast is occupied by dunes. They form a natural flood and erosion barrier against marine processes. It is estimated that at the beginning of the 21st century the mean rate of shore recession for the entire Polish coast was in the range of 1–2 m/year, and now it tends to increase. The government will therefore have to spend more money on coastal protection from erosion and floods (currently, it is over £ 10 million of Polish taxpayers' money per year, cf. *Journal of Laws* 2015, No. 0, item 1700, plus ca. £ 100 million obtained from the EU between 2004 and 2015). Moreover, it is expected that large infrastructural projects (such as a nuclear power plant, wind farms and a major gas pipeline from Norway and Denmark to Poland) will be located on dune coastal segments in coming decades. Some of the basic parameters necessary for the future planning of seashore protection and coastal flood risk assessment are the dune erosion rate and the probability of dune breaching under conditions of storm surges. A number of analytical and numerical models have been developed to determine these parameters.

* This paper is dedicated to the memory of Professor Zbigniew Pruszak (1947–2018).

2. Research Goal

The practical goals of this study, based on in-situ measurements carried out under natural conditions at the Coastal Research Station Lubiatowo, included the adaptation and preliminary verification of the numerical model *Xbech* for calculating the erosion of dunes affected by extreme hydrodynamic phenomena.

3. State of the Art

The first computations of the rate of natural dune abrasion were done in the 1960s. Bruun (1962) proposed a method for the assessment of beach retreat as a function of seawater level rise, which was based on the beach equilibrium concept. According to the assumptions of this method, after a sufficiently long impact of a high seawater level, the cross-shore profile ultimately recedes, and the eroded material is deposited lower along the profile to satisfy the mass balance. In this approach, horizontal changes in beach position are directly proportional to seawater level. The Bruun model was developed by Edelman (1972). The model equations require prior determination of the active dune profile width, the depth of the seabed at wave breaking before and after a storm, and the dune height relative to the mean sea level. Dean and Maurmeyer (1983) presented a model in which a dimensionless beach retreat can be evaluated based on the storm surge and the depth of the seabed at wave breaking. The difference between this approach and previous models consisted in the fact that the previous models assumed an instantaneous rise in seawater level and a somewhat delayed formation of a new equilibrium profile. It produced a vertical slope of the equilibrium profile at the sea-land interface, whereas in Maurmeyer's approach the shape of the equilibrium profile in that region was close to a triangular one. Vellinga (1986) further developed this model, whereas van de Graaff (1986) adapted it to a probabilistic design concept of dune heights on the Dutch coast. Next, Kobayashi (1997) proposed a model combining the mass conservation principle in the nearshore zone with empirical formulas of sediment transport. As a result, a partial differential equation was defined that could be solved for a simple nearshore geometry. Kriebel et al (1991) presented an analytical model that described the volume of sediment eroded from the dune as a function of the storm surge and dune geometry (dune height, dune foot elevation with respect to the mean sea level and dune crest width). In this model, the rise in seawater level that triggers dune erosion.

All the above models assumed that the rise in seawater level occurs discretely and remains constant during the entire storm. The material eroded from the dune is deposited on the cross-shore profile near the wave breaking location that corresponds to mean sea level conditions. Most of those models also assumed that the receding dune face takes a vertical shape, and the corresponding cross-shore profile tends towards a new equilibrium. Under natural conditions, morphological changes are much slower than their hydrodynamic forcing, and a storm rarely lasts long enough to form a new equilibrium profile. An example of this approach was the Dutch model *DUNE*,

adapted to Polish conditions to assess the safety of dune coastal segments from the mid-1990s onwards. This model, as well as all other based on the equilibrium profile concept, overestimates the rates of dune erosion with respect to actual depletions.

A different approach was presented by Fisher and Overton (1984) and by Nishi and Kraus (1996). Their models assume that the total dune erosion results from a sum of impacts of waves running up the beach during a storm. Thus, over a storm period, erosion depends on the frequency and energy flux of individual waves. This phenomenon was described mathematically as momentum transfer after wave contact with the dune face. The volume of sediment eroded by a single wave was assessed by laboratory tests in wave flumes (Overton et al 1987, 1990, 1994). The analytical model by Larson et al (2004), calculating dune erosion during storms, sums up the study by Fisher and Overton (1984). Practical applications of this model require determination of empirical coefficients, adequate for coastal segments under study.

The latest approach to the modelling of dune erosion is represented by the *XBeach* model. It was tested in the Great Flume in Delft (Roelvink et al 2009, van Thiel de Vries 2009) and under natural conditions (Roelvink et al 2009). It is currently widely used for computations of foreshore and backshore evolution of dune coasts (Vousdoukas et al 2011, Harley et al 2011, Bolle et al 2011, Bugajny 2013, 2015, Furmańczyk et al 2014, Szmytkiewicz et al 2017).

4. Description of the *Xbeach* model

The basic modules of the *Xbeach* model (Roelvink et al 2010) necessary to calculate morphological changes in the nearshore and backshore zones during storm conditions are as follows:

- the wave module, in which wave transformation and wave breaking in the coastal zone are calculated from the energy flux conservation equation (wave motion equation),
- the current module, in which the velocity field and water flow directions in the coastal zone are calculated using the solution of mass and momentum conservation equations
- the bedload transport module, in which the solution of the advection-diffusion equation leads to the calculation of sediment concentration, sediment transport and morphological changes in the coastal zone,
- the seabed rework module.

4.1. The Wave Module

The main equation describing the wave action balance is

$$\frac{\partial A}{\partial t} + \frac{\partial c_x A}{\partial x} + \frac{\partial c_y A}{\partial y} + \frac{\partial c_\theta A}{\partial \theta} = -\frac{D_w + D_f}{\sigma}, \tag{1}$$

where:

$$A(x, y, t, \theta) = \frac{S_w(x, y, t, \theta)}{\sigma(x, y, t)}, \tag{2}$$

$$S_w = \frac{1}{8}\rho\, g\, H^2, \tag{3}$$

$$\sigma = \frac{2\pi}{T}, \tag{4}$$

t, x, y and θ are, respectively, time, distance along the OX axis (perpendicular to the seashore), distance along the OY axis (parallel to the seashore), and wave approach angle; H and T are wave height and period, ρ is water density, and g is the gravitational acceleration.

The wave action propagation speeds x, y and directional space are given by

$$\begin{aligned} c_x &= c_g \cos\theta, \\ c_y &= c_g \sin\theta, \\ c_\theta &= \frac{\sigma}{\sinh 2kh}\left(\frac{\partial h}{\partial x}\sin\theta - \frac{\partial h}{\partial y}\cos\theta\right), \end{aligned} \tag{5}$$

where h represents the local water depth, and k is the wave number.

The wave action A in this description is not only a function of time and horizontal variables in the OXY plane, but it also depends on the angle of wave approach θ and the angular frequency of the wave σ. This means that at a given moment of time, at a given point of the XY grid, we are dealing with a wave energy distribution that depends on the wave approach angle.

The rate of wave energy dissipation is determined by the sum of dissipation resulting from wave breaking and bottom friction. The rate of energy dissipated by breaking waves D_w is determined according to works by Battjes and Janssen (1978), and the final formula was developed by Baldock et al (1998):

$$D_w = \frac{1}{4}\alpha\, Q_b\, \rho\, g\, f_{rep}\, (H_b + H_{rms}), \tag{6}$$

where:

$$Q_b = \exp\left(-\frac{H_b^2}{H_{rms}^2}\right), \tag{7}$$

$$H_b = \frac{0.88}{k}\tanh\left(\frac{\gamma\, k\, h}{0.88}\right), \tag{8}$$

α – empirical coefficient of order 0 (1),

Q_b – factor describing the percentage of broken waves and waves collapsing at a given point,

H_b – the maximum height of a wave breaking at a given point,
k – wave number,
h – depth,
γ – wave breaking coefficient,
f_{rep} – average wave frequency.

The second component of dissipation is the bottom friction expressed by the function

$$D_f = \frac{2}{3\pi}\rho f_w \left(\frac{\pi H_{rms}}{T \sinh(k h)}\right)^3, \tag{9}$$

where f_w is a friction factor.

The model also includes a dissipation factor related to friction against a vegetated seabed.
In addition to these parameters, radiation stresses are calculated:

$$\begin{aligned} S_{xx}(x,y,t) &= \int \left(\frac{c_g}{c}\left(1+\cos^2\theta\right)-\frac{1}{2}\right) S_w d\theta, \\ S_{xy}(x,y,t) = S_{yx}(x,y,t) &= \int \sin\theta\cos\theta\left(\frac{c_g}{c}\right) S_w d\theta, \\ S_{yy}(x,y,t) &= \int \left(\frac{c_g}{c}\left(1+\sin^2\theta\right)-\frac{1}{2}\right) S_w d\theta, \end{aligned} \tag{10}$$

based on which wave energy (power) is calculated:

$$\begin{aligned} F_x(x,y,t) &= -\left(\frac{\partial S_{xx}}{\partial x}+\frac{\partial S_{xy}}{\partial y}\right), \\ F_y(x,y,t) &= -\left(\frac{\partial S_{xy}}{\partial x}+\frac{\partial S_{yy}}{\partial y}\right), \end{aligned} \tag{11}$$

which is a link to the next stage, that is, the calculation of wave-induced currents.

Equation (1) is solved using Euler's explicit numerical scheme (Euler's method). The calculations yield the following values for each node of the numerical grid: wave heights, mean wave-approach azimuths, spatial and directional distribution of wave energy, group and phase velocities, the rate of wave energy dissipation as a result of wave refraction (wave breaking), bottom friction, and radiation stresses.

4.2. The Current Module

The current module calculates wave-induced currents in the coastal zone, where waves transform and break, starting from a depth smaller than half the wavelength. This transformation and breaking of waves generates new forms of wave motion, such as wave-induced currents.

In calculating the water flow velocity, the *Xbeach* model assumes that the total water movement of wind-generated waves can be expressed as the sum of the wave-induced current as well as orbital and turbulent velocities:

$$u_i = u_{ip} + \widetilde{u}_i + u_i' \tag{12}$$

and that the vertical component (assuming there is no average water flow velocity w_p) can be expressed as the sum of orbital velocities and pulsations:

$$w = \widetilde{w} + w', \tag{13}$$

where:

$i = 1, 2,$

u_{ip} – low-frequency components of water flow whose averaging periods are significantly longer than the wave period,
$\widetilde{u}_i, \widetilde{w}$ – oscillatory (orbital) velocities associated with the presence of wave motion,
u', w' – turbulent fluctuations.

When scalar products of velocities $(u_i u_j)$ $(i, j = 1, 2)$ and $(u_i w)$ $(i = 1, 2)$ are averaged over time T_1 and averaging periods are much larger than periods of pulsation and much smaller than wave periods, one can assume in the first approximation (due to different sources of velocity components) that there is no correlation between the following moments:

$$\begin{aligned} \left\langle u_{ip} u_i' \right\rangle &= u_{ip} \left\langle u_i' \right\rangle = 0, \\ \left\langle u_{ip} w' \right\rangle &= u_{ip} \left\langle w' \right\rangle = 0, \\ \left\langle \widetilde{u}_{ip} u_i' \right\rangle &\approx \widetilde{u}_{ip} \left\langle u_i' \right\rangle = 0, \\ \left\langle \widetilde{w} u_i' \right\rangle &\approx \widetilde{w} \left\langle u_i' \right\rangle = 0, \end{aligned} \tag{14}$$

where:

$\langle\rangle$ – averaging over time T_1,
T_1 – averaging period that meets the condition $T_{turb} \ll T_1 \ll T$,
T_{turb} – period of turbulent velocity pulsation,
T – wave period.

Using the assumption of the generalized Lagrangian mean (GLM) (Andrews and McIntyre 1978, Walstra et al 2000), the conservation of momentum and mass can be expressed by the following equations:

$$\begin{aligned}
&\frac{\partial u^L}{\partial t} + u^L\frac{\partial u^L}{\partial x} + v^L\frac{\partial u^L}{\partial y} - fv^L - \upsilon_h\left(\frac{\partial^2 u^L}{\partial x^2} + \frac{\partial^2 u^L}{\partial y^2}\right) = \\
&\qquad \frac{\tau_{sx}}{\rho h} - \frac{\tau^E_{bx}}{\rho h} - g\frac{\partial \eta}{\partial x} + \frac{F_x}{\rho h}, \\
&\frac{\partial v^L}{\partial t} + u^L\frac{\partial v^L}{\partial x} + v^L\frac{\partial v^L}{\partial y} - fu^L - \upsilon_h\left(\frac{\partial^2 v^L}{\partial x^2} + \frac{\partial^2 v^L}{\partial y^2}\right) = \\
&\qquad \frac{\tau_{sy}}{\rho h} - \frac{\tau^E_{by}}{\rho h} - g\frac{\partial \eta}{\partial y} + \frac{F_y}{\rho h},
\end{aligned} \tag{15}$$

$$\frac{\partial \eta}{\partial t} + \frac{\partial h u^L}{\partial x} + \frac{\partial h v^L}{\partial y} = 0, \tag{16}$$

where:

f – the Coriolis coefficient (parameter),
υ_h – the coefficient of viscosity calculated from the Smagorinsky model [20],
τ_{sx}, τ_{sy} – shear stresses on the water surface associated with the presence of wind,
τ_{bx}, τ_{by} – bottom shear stresses,
η – free water surface elevation,
index ^{L} – Lagrangian velocity,
index ^{E} – Eulerian velocity.

The values of stresses τ_s on the water surface are determined as a function of wind velocity using classical equations:

$$\begin{aligned}
\tau_{sx} &= \rho_a\, C_d\, W\, |W_x|\,, \\
\tau_{sy} &= \rho_a\, C_d\, W\, |W_y|\,,
\end{aligned} \tag{17}$$

where:

ρ_a – air density,
C_d – coefficient of air resistance,
W – wind velocity.

The value of bottom shear stresses τ_b is calculated from the formula

$$\begin{aligned}
\tau^E_{bx} &= c_f\, \rho\, u^E \sqrt{(1.16\, u_{rms})^2 + (u^E)^2 + (v^E)^2}, \\
\tau^E_{by} &= c_f\, \rho\, v^E \sqrt{(1.16\, u_{rms})^2 + (u^E)^2 + (v^E)^2},
\end{aligned} \tag{18}$$

where:

u_{rms} – mean-square maximum bottom orbital velocity,
c_f – coefficient of bottom friction.

Lagrangian velocities are associated with Eulerian velocities through the following relations:

$$\begin{aligned} u^L &= u^E + u^S, \\ v^L &= v^E + v^S, \end{aligned} \tag{19}$$

where the index S denotes the Stokes drift:

$$u^S = \frac{E \cos\theta}{\rho h c}, \tag{20}$$

$$v^S = \frac{E \sin\theta}{\rho h c}, \tag{21}$$

where:

$E = \rho g H^2/8$ – wave energy,
c – phase velocity of a wave,
h – water depth
θ – wave approach angle to the shoreline.

4.3. The Bedload Transport Module

The volume of sediment transport is described by the advection-diffusion equation averaged over the depth and wave period:

$$\frac{\partial hC}{\partial t} + \frac{\partial hCu^E}{\partial x} + \frac{\partial hCv^E}{\partial y} + \frac{\partial}{\partial x}\left(D_h h \frac{\partial C}{\partial x}\right) + \frac{\partial}{\partial y}\left(D_h h \frac{\partial C}{\partial y}\right) = \frac{hC_{eq} - hC}{T_s}, \tag{22}$$

$$T_s = \max\left(0.05\frac{h}{w_s}; 0.02\right), \tag{23}$$

where:

C – the concentration of sediments averaged over the depth and wave period,
D_h – the sediment diffusion coefficient,
T_s – the so-called adaptation time expressed as a function of sediment particles settling at the bottom.

The adaptation time T_s is the time required for sediment particles to travel at a depth of $0.05h$, and it should not be less than 0.02 sec.

C_{eq} is the so-called equilibrium concentration described by the Soulsby-van Rijn [21] equation:

$$C_{eq} = \frac{A_{sb} + A_{ss}}{h}\left[\left(\left|u^E\right|^2 + 0.018\frac{u_{rms}^2}{C_d}\right)^{0.5} - u_{cr}\right]^{2.4}(1 - \alpha_b\, m)\,, \tag{24}$$

where:

- $A_{sb},\ A_{ss}$ – coefficients of dragged and suspended sediments (respectively), which are a function of grain diameter, sediment density and water depth,
- u_{rms} – maximum bottom orbital velocity,
- C_d – coefficient of resistance,
- u_{cr} – threshold (critical) velocity above which the bedload transport begins,
- $(1 - \alpha_b\, m)$ – correction of the concentration equilibrium related to the seabed slope (gradient),
- m – seabed slope,
- α_b – calibration coefficient.

The equilibrium concentration C_{eq} refers to a concentration that does not change under specific local hydrodynamic, bathymetric and morphological conditions – in other words, the same amount of sediment is settled to and lifted from the bottom. When the actual concentration is greater than the C_{eq} value, more sediment settles on the bottom than is lifted, and the concentration decreases over time (towards the equilibrium concentration). When the actual concentration is lower that the C_{eq} value, more sediment particles are lifted compared to particles settling to the bottom. With constant hydrodynamic forces, the actual concentration of sediments is aimed at the equilibrium concentration.

4.4. Seabed Reworking

The relationship between seabed reworking at a given time and the rate of onshore, offshore and longshore sediment transport is described in a general form by the continuity equation for sediment, the so-called 1-line equation:

$$\frac{\partial z_b}{\partial t} + \frac{f_{mor}}{(1-p)}\left(\frac{\partial q_x}{\partial x} + \frac{\partial q_y}{\partial y}\right) = 0, \tag{25}$$

where:

- z_b – seabed level,
- p – porosity of the ground,
- f_{mor} – correction factor "accelerating" the calculated bathymetric changes.

If, for example, we adopt the factor $f_{mor} = 10$ and assume 6 minutes as a simulation time, the calculated bathymetric changes will correspond to a simulation time of 1 hour. To obtain fully reliable results, the factor $f_{mor} = 1$ should be used. This, however, means a considerably longer calculation time. Determination of the optimal value of the factor f_{mor} for a specific stretch of the seashore requires calibration of the *Xbeach* model.

The sediment transport rates q_x (in the direction perpendicular to the shore) and q_y (parallel to the shore) are determined from the following equations:

$$\begin{aligned} q_x(x,y,t) &= \left(\frac{\partial(h\,C\,u^E)}{\partial x}\right) + \left(\frac{\partial}{\partial x}\left(D_h\,h\frac{\partial C}{\partial x}\right)\right), \\ q_y(x,y,t) &= \left(\frac{\partial(h\,C\,tv^E)}{\partial y}\right) + \left(\frac{\partial}{\partial y}\left(D_h\,h\frac{\partial C}{\partial y}\right)\right). \end{aligned} \tag{26}$$

4.5. Dune Reworking

The *Xbeach* model makes it possible to calculate changes (reworking) in the backshore (beach and dune), that is, to "extend" computations beyond the permanently inundated area. This means that the calculations of shoreline profile changes (reworking) are not limited to the last node of the numerical grid located under water, but the calculated depth changes affect elevation changes in grid nodes located above water. The calculations are performed using a relatively simple mechanism in the model, referred to as avalanching.

In the dune remodelling module, the first step calculates the amount of run-up on the beaches, and the dune profile is computed. During the calculations, the model checks whether, for a given time step, the currently determined new relief does not exceed the permissible maximum slope angle:

$$\left|\frac{\partial z_b}{\partial x}\right| > m_{cr}. \tag{27}$$

If the slope is too steep, an "avalanche" occurs, that is, the slope collapses and slides down in such a way that the new slope inclination does not exceed the permissible angle. The critical bed slope is a user-defined parameter ranging from 0.1 to 2.0 for dry sand and from 0.1 to 1.0 for wet sand. The slope sliding consists in calculating the elevation change for the terrain:

$$\Delta z_b = \min\left[\left(\left|\frac{\partial z_b}{\partial x}\right| - m_{cr}\right)\Delta x\,;\ 0.05\,\Delta t\right] \tag{28}$$

and then adding this change to or subtracting it from two grid nodes forming a steep slope.

$$\begin{aligned} z_{b\,i,j}^{t+1} &= z_{b\,i,j}^{t} + \Delta z_{b\,i,j}, \\ z_{b\,i+1,j}^{t+1} &= z_{b\,i+1,j}^{t} - \Delta z_{b\,i,j}. \end{aligned} \tag{29}$$

The change in elevation is subtracted from the higher node and added to the lower one so that after the operation the inclination of the slope decreases by $2\Delta z_b$.

The value of $0.05\Delta t$ in formula (28) is added artificially so that the calculated changes in the elevation of the backshore are not too abrupt.

5. Study area

The research was conducted on a sand dune located in the vicinity of the Coastal Research Station (CRS) of the Institute of Hydro-Engineering, Polish Academy of Sciences (IBW PAS) in Lubiatowo (Gmina Choczewo, Pomeranian Voivodeship – Fig. 1).

Fig. 1. Location of the Coastal Research Station (CRS) in Lubiatowo

The seashore in this area is characterised by a gentle inclination of the seabed (≈ 0.015) and is built of fine-grained quartz sand with an average grain diameter of $D_{50} \sim 0.22$ mm. There are 3–4 stable submerged sandbars in the surveyed coastal area. Their distances from the shoreline are 80–120 m for the first sandbar, 170–230 m for the second, and 300–380 m for the third, while the fourth and possibly the fifth sandbar usually form one larger unstable landform at a distance of 650–850 m from the shore. In addition to quasi-stable sandbars, one ephemeral sandbar in the form of a flat underwater shoal continuously migrating sea- or shorewards has been observed in the study area at a depth of ca. 1 m (about 50 m from the shore) (Szmytkiewicz and Zabuski 2017). The calculations of dune profile changes were performed in six measured profiles spaced every 100 m, referred to as profiles no. 03, 04, 05, 06, 07 and 08 (Fig. 2).

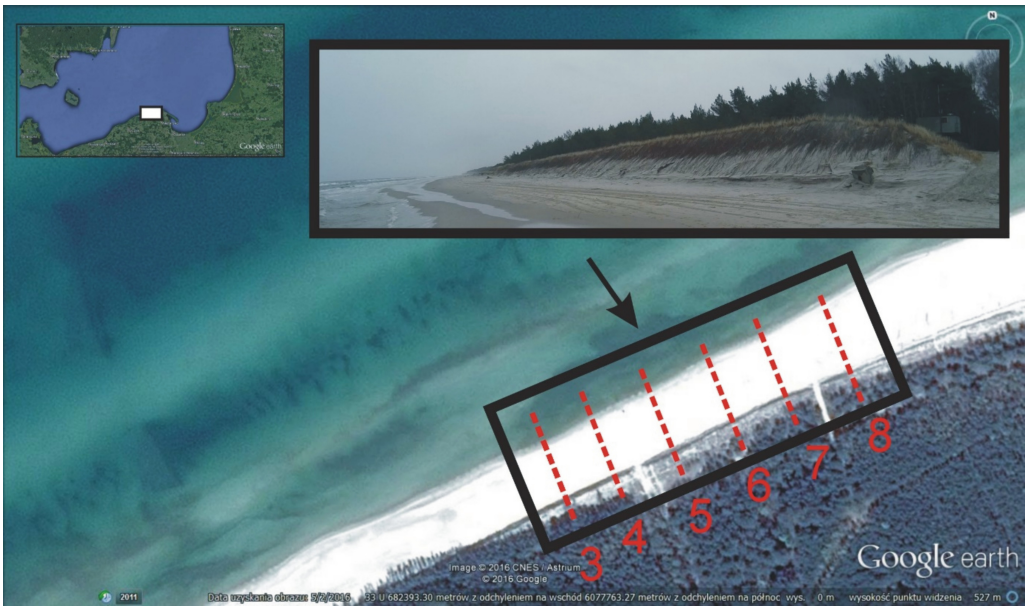

Fig. 2. The vicinity of the Coastal Research Station in Lubiatowo (CRS): the dune and the profiles under analysis

The dune system of the shore under analysis is built of sand with a grain diameter ranging from 0.16 to 0.25 mm. As a result of selection during sediment transport, finer and more rounded sediment grains reach the dune ridge, while depressions contain coarser aeolian material. A significant part of this seashore stretch is covered by aeolian deposits from 2 to 3 m in height. In the eastern part of the study area, irregular dune elevations with height differences ranging from 10 to 20 m ASL are located. The base of irregular elevations is located at an altitude of 1–2 m ASL. The width of the beach is up to 50 m along devastated stretches and more than 50 m within depositional sections. There are three generations of dunes along the depositional stretches: the oldest stabilised dune overgrown with forest, the younger, partly stabilised dune and the frontal dune, currently being formed. In order to protect the shores, biological reinforcement has been implemented – for example, fascine fences and dune consolidation by planting sand ryegrass (Łabuz 2005).

In the study area, Paleogene and Neogene sediment strata, deposited in the Quaternary substratum (Skompski 1985), are represented by siltstone, silt, clay and silty sands with glauconite from the upper Eocene and the Oligocene as well as miocene silts and sands with interlayers of clay and thin partings of brown coal. Within the land area, boulder clay of the North Poland glaciation is deposited below 10 m BSL. They are overlain by a series of Pleistocene fluvioglacial sand deposits represented by calcareous sands with an admixture of gravel characterised by varying particle size distribution and containing marine fauna. A layer of these deposits is also present in

the nearshore zone, where it forms a substratum for marine sands at a depth of 7–8 m MSL.

6. Results of Computations

To calculate sand dune abrasion in the CRS area, the numerical *Xbeach* model was used along with measurement data recorded before, during and after Hurricane Ksawery, which occurred on December 6–8, 2013.

6.1. Description of Hurricane Ksawery

A strong low-pressure area was formed over the North-West Atlantic and the North Sea, which moved eastwards and reached the Southern and Central Baltic on December 6–8, 2013. This low-pressure system, resulting from a rapid drop in atmospheric pressure in its central part, caused rapid north-western air circulation with very strong winds. The wind velocity was of the order of 25 m/s. During the hurricane, the beach was inundated with water.

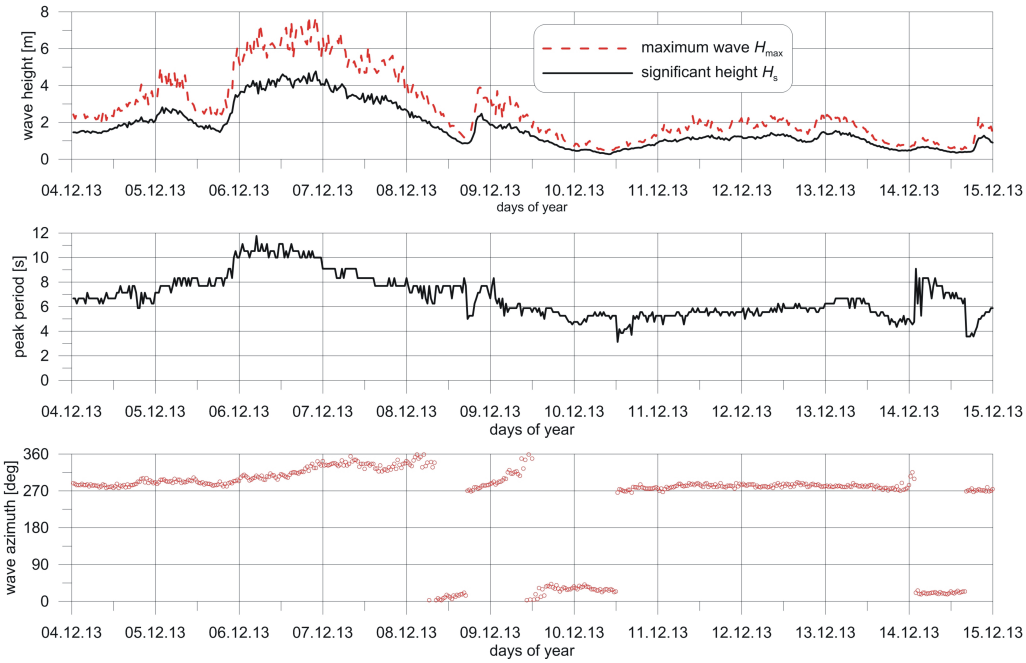

Fig. 3. Parameters of waves measured at a depth of about 20 m in the vicinity of CRS Lubiatowo at the time of Hurricane Ksawery on the Baltic Sea

Wind-generated waves in the first decade of December, associated with Hurricane Ksawery, were characterised by the occurrence of three consecutive storms. The first one, with a significant wave height of H_s = 2–3 m and the maximum wave height

$H_{\max}$ ranging from 4 to 5 m, took place on the night of December 4–5. The second (strongest) storm, which took place on December 6–8, was characterised by significant waves of H_s = 4–5 m and maximum waves of $H_{\max}$ = 6–8 m. The third one, which occurred on the night of December 9–10, was milder, with heights of $H_s \approx 2$ m and $H_{\max}$ = 3–4 m. Throughout this period, most waves approached the seashore from the northern direction, which means that they were almost perpendicular to the shore. Fig. 3 shows parameters of deep-water waves measured by a wave buoy at a depth of approximately 20 m between December 4 and December 14, 2013.

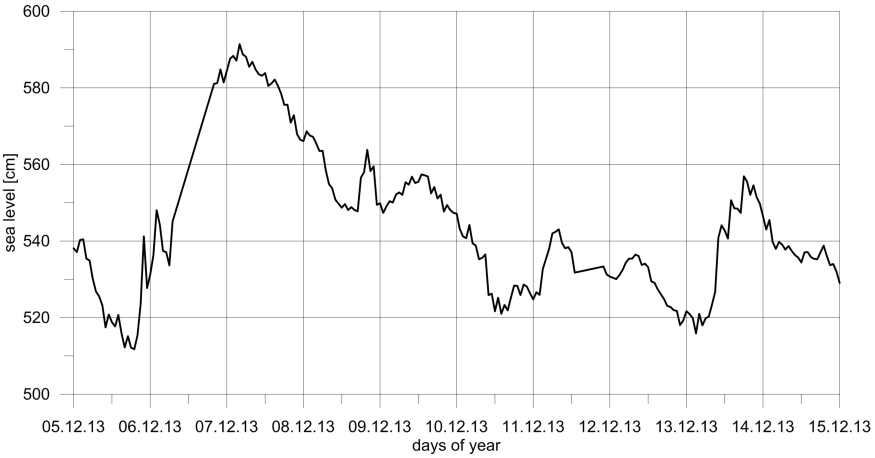

Fig. 4. Water levels in the vicinity of CRS Lubiatowo during Hurricane Ksawery on the Baltic Sea

Fig. 4 shows averaged water levels for the same period, measured in Łeba and Władysławowo. By comparing water levels measured in the previous years at CRS Lubiatowo with those measured in the two above-mentioned ports, it was found that water levels in Lubiatowo can be calculated as a weighted average of those measured in Łeba (65%) and Władysławowo (35%). It appears from Fig. 4 that the maximum water level was 540 cm during the first storm, 590 cm during the second, strongest storm, and about 560 cm during the third.

6.2. Calculations

Calculations of dune profile changes for December 4–14, 2013, were performed using the *Xbeach* numerical model. At the seaward limit of each bathymetric-tachymetric profile (at a depth of about 20 m), statistical deep-water parameters of waves (significant wave height, peak period, wave approach angle azimuth) and water levels were defined for each hour (Figs. 3 and 4), and then wave-to-shore transformation and dune destruction were calculated. The time step of the calculations Δt was determined automatically on the basis of the pre-set values of Δx and Δy, so that the Courant number was not higher than 0.35 s.

Beach profiles from 2013 combined with dune profiles from 2012 were included in the calculations as initial tachymetric profiles 03–08. Beach profiles from January 2014 were used as the final measured profiles and were compared with the calculated beach profile changes and dune erosion after Hurricane Ksawery. After the hurricane, the width of the beach was measured from the shoreline to the foot of the dune. The ordinate crests of the dunes in the period from 2012 to the end of 2013 did not change. The seabed bathymetry used in the calculations came from survey measurements conducted on July 4, 2013.

The calculated and measured changes in beach and dune profiles caused by Hurricane Ksawery are compared in Figs 5a–5f.

The comparisons of the calculated and measured changes in the beach topography and dune foot position (presented in the above figures) show that:

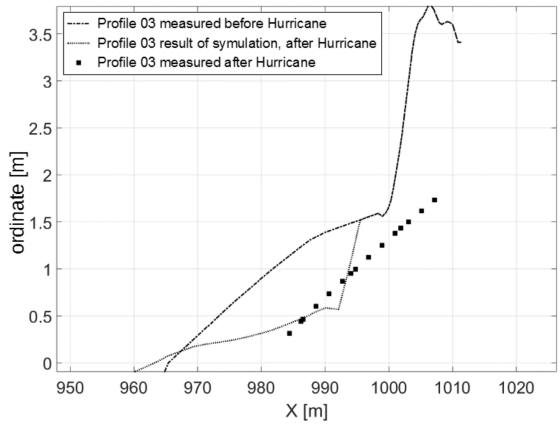

Fig. 5a. Comparison of the calculated and measured changes in beach and dune profiles during Hurricane Ksawery for Profile 03

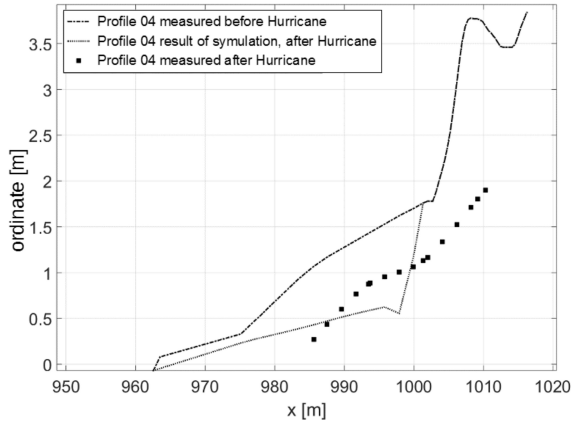

Fig. 5b. Comparison of the calculated and measured changes in beach and dune profiles during Hurricane Ksawery for Profile 04

– the actual dune recession for profiles 03, 04, 05, 06, 08, ranging from 10 to 16 m, was greater than the calculated values of 2–13 m,
– the calculated and actual dune destruction values were similar for profile 07.

7. Conclusions

The results presented in Fig. 5a–f show that beach erosion was calculated properly, which indicates that the adopted dune avalanche model is correct. In contrast, the process of washing out of sandy sediment is clearly underrated, which can probably be attributed to the underrated run-down velocity.

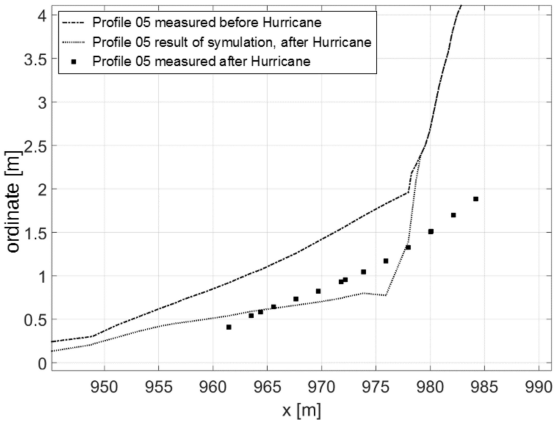

Fig. 5c. Comparison of the calculated and measured changes in beach and dune profiles during Hurricane Ksawery for Profile 05

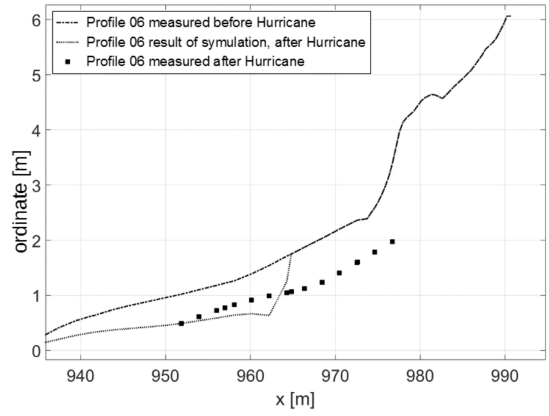

Fig. 5d. Comparison of the calculated and measured changes in beach and dune profiles during Hurricane Ksawery for Profile 06

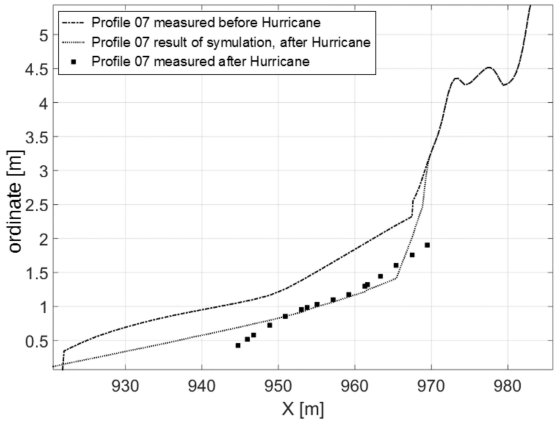

Fig. 5e. Comparison of the calculated and measured changes in beach and dune profiles during Hurricane Ksawery for Profile 07

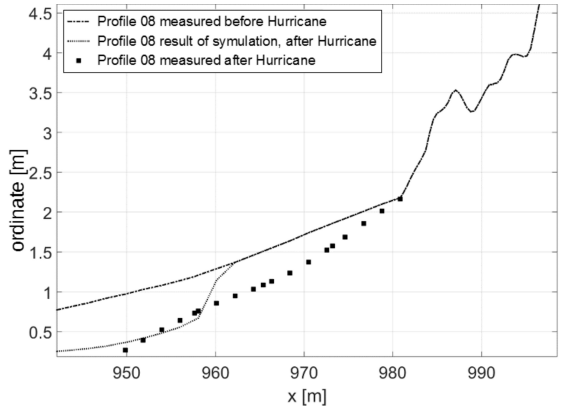

Fig. 5f. Comparison of the calculated and measured changes in beach and dune profiles during Hurricane Ksawery for Profile 085

Long-term observations of dune destruction during storms reveal that wave attacks on the dune foot produce landslide phenomena in the upper part of the dune massif, which has no direct contact with the waves. This phenomenon is not accounted for during computations. It appears that proper modelling of dune erosion should include an accurate mapping of wave attack against the dune foot and the generation of pore water pressure inside the dune massif, which lead to the loss of dune stability and landslide phenomena.

Acknowledgments

The investigations presented in this paper were supported and conducted by the National Science Centre, Poland, under the research project *Wave run-up phenomena:*

Adaptation and verification of existing mathematical models. Determination of empirical formula for southern Baltic Sea coast, contract number 2016/21/N/ST8/02390, and mission-related activities of IBW PAN, financed by the Polish Ministry of Science and Higher Education.

References

Andrews D. G., McIntyre M. E. (1978) An exact theory of nonlinear waves on a Lagrangian-mean flow, *Journal of Fluid Mechanics*, **89**, 609.

Baldock T. E., Holmes P., Bunker S., van Weert P. (1998) Cross-shore hydrodynamics within an unsaturated surfzone, *Coastal Engineering*, **34**, 173–196.

Battjes J. A., Janssen J. P. F. M. (1978) Energy loss and set-up due to breaking of random waves, *Proc. 16th Conf. CoastalEng.*, vol. I, 569-587.

Bolle A., Mercelis P., Roelvink D., Haerens P., Trouw K. (2011) Application and validation of XBeach for three different field sites. [in:] Smith J. K., Lynnet P. (Eds.), *Proceedings 32nd Conference on Coastal Engineering (Shanghai, China)*, Coastal Engineering, Special Issue No. 32, sediment.40.

Bruun P. (1962) Sea level rise as a cause of shore erosion, *Journal of Waterways and Harbors Division*, **88** (1), 117–130.

Bugajny N., Furmańczyk K., Dudzińska-Nowak J., Paplińska-Swerpel B. (2013) Modelling morphological changes of beach and dune induced by storm on the Southern Baltic coast using XBeach (case study: Dziwnow Spit), [in:] Conley D. C., Masselink G., Russell P. E. and O'Hare T. J. (Eds.), *Proc. 12th International Coastal Symposium (Plymouth, England)*, Journal of Coastal Research, Special Issue No. 65, 672–677.

Bugajny N., Furmańczyk K., Dudzińska-Nowak J. (2015), Application of XBeach to model storm response on a sandy spit at the southern Baltic, *Oceanological and Hydrological Studies* (manuscript in preparation).

Dean R. G., Maurmeyer E. M. (1983) Models for beach profile response, [in:] Komar P. (Ed.) *Handbook of Coastal Processes and Erosion*, CRC Press, Boca Ranon, 151–165.

Edelman T. (1972) Dune erosion during storm conditions, *Proceedings of the 13*th *Coastal Engineering Conference*, ASCE, 1305–1311.

Fisher J. S., Overton M. F. (1984) Numerical model for dune erosion due to wave uprush, *Proceedings of the 19*th *Coastal Engineering Conference ASCE*, 1553–1558.

Furmańczyk K., Andrzejewski A., Benedyczak R., Bugajny N., Cieszyński Ł., Dudzińska-Nowak J., Giza A., Paprotny D., Terefenko T., Zawiślak T. (2014) Recording of selected effects and hazards from current and expected storm events at the Baltic Sea coastal zone, [in:] Green A. N. and Cooper J. A. G. (Eds.), *Journal of Coastal Research*, Special Issue No. 70, 338–342.

Harley M., Armaroli C., Ciavola P. (2011) Evaluation of XBeach predictions for a real-time warning system in Emilia-Romagna, Northern Italy, [in:] Furmańczyk K. (Ed.), *Proceedings 11th International Coastal Symposium*, (Szczecin, Poland), Journal of Coastal Research, Special Issue No. 64, 1861–1865.

Kobayashi N. (1997) *Wave runup and overtopping on beaches and coastal structures*, Research Report No. CACR-97-09, Newark, DE, University of Delaware, Center for Applied Coastal Research.

Kriebel D. L., Kraus N. C., Larson M. (1991) Engineering methods for cross-shore beach profile response, *Proceedings of Coastal Sediments 91*, ASCE, 557–571.

Łabuz T. A. (2005) Brzegi wydmowe polskiego wybrzeża Bałtyku (Dune shores of Polish Baltic coast), *Czasopismo Geograficzne*, **76** (1–2), 19–47.

Larson M., Erikson L., Hanson H. (2004) An analytical model to predict dune erosion due to wave impact, *Coastal Engineering*, **51**, 675–696.

Nishi R., Kraus N. C. (1996) Mechanism and calculation of sand dune erosion by storms, *Proceedings of the 25th Coastal Engineering Conference*, ASCE, 3034–3047.

Overton M. F., Fisher J. S., Fenaish T. (1987) Numerical analysis of swash forces on dunes, *Proceedings of the 22nd Coastal Engineering Conference*, ASCE, 2471–2479.

Overton M. F., Fisher J. S., Stone A. L. (1990) Large scale laboratory tests of dune erosion, *Proceedings of the 22nd Coastal Engineering Conference*, ASCE, 2471–2479.

Overton M. F., Pratikto W. A., Lu J. C., Fisher J. S. (1994) Laboratory investigation of dune erosion as a function of sand grain size and dune density, *Coastal Engineering*, **23**, 2471–2479.

Roelvink D., Reniers A., van Dongeren A., van Thiel de Vries J., Lescinski J., McCall R. (2010) *XBeach Model Description and Manual*, Unesco-IHE Institute for Water Education, Deltares and Delft University of Technology, version 6, 1–106.

Roelvink, D., Reniers, A., van Dongeren, A., van Thiel de Vries J., McCall R., Lescinski J. (2009) *Modelling storm impacts on beaches dunes and barrier islands*, *Coastal Engineering*, **56** (11–12), 1133–1152.

Skompski S. (1985) *Szczegółowa mapa geologiczna Polski w skali 1:50 000 wraz z objaśnieniami. Arkusz Choczewo*, PIG, Warszawa (in Polish).

Soulsby R. L. (1997) *Dynamics of Marine Sands*, London, Thomas Telford Publications.

Szmytkiewicz P., Zabuski L. (2017) Analysis of dune erosion on the coast of south Baltic Sea with taking into account dune landslide processes, *Archives of Hydro-Engineering and Environmental Mechanics*, **64** (1), 3–16.

Van de Graaff J. (1986) Probabilistic design of dunes; an example from the Netherlands, *Coastal Engineering*, **9**, 479–500.

Van Thiel de Vries J. S. M. (2009) *Dune erosion during storm surges*, Amsterdam, Netherlands, IOS Press, 202 p.

Vellinga P. (1986) *Beach and dune erosion during storm surges*, PhD thesis, Delft Hydraulics Communications No 372, Delft Hydraulics Laboratory, Delft, The Netherlands.

Vousdoukas M. I., Almeida L. P., Ferreira Ó. (2011) Modelling storm-induced beach morphological change in a meso-tidal, reflective beach using XBeach, [in:] Furmańczyk K. (Ed.), *Proc. 11th International Coastal Symposium*, (Szczecin, Poland), Journal of Coastal Research, Special Issue No. 64, 1916–1920.

Walstra D. J. R., Roelvink J. A., Groeneweg J. (2000) Calculation of wave-driven currents in a 3D mean flow model, *Proceedings of the 27th International Conference on Coastal Engineering*, 1050–1063.